

## Injection locking of a long-pulse relativistic magnetron

S.C. Chen, G. Bekefi, and R.J. Temkin

Massachusetts Institute of Technology  
Cambridge, MA 02139

### Abstract

We report the injection locking results of a long-pulse (200–400 ns) high power (20–30 MW) relativistic magnetron at 3.3 GHz. Phase-locking with reproducible locked angle is achieved with an injection power ratio as low as 1:200. The locked states are phase stable to within  $\pm 3^\circ$  during the pulse. Phase locking physics is studied and important effects due to frequency pushing are identified. The locking bandwidth and the dependence of final locked phase on injection parameters are measured and are found to agree well with theory.

### I. INTRODUCTION

Phase-locking of a high power relativistic magnetron oscillator has been a subject of intensive experimental<sup>1–5</sup> and theoretical research.<sup>6–9</sup> Phase locking through the injection of an external low power reference signal has the following advantages. First, the same phase locking physics applies to all the master-slave pairs and to the whole phase-locked array. No additional complication arises for phase-locking a large number of oscillators. Second, output phase and frequency can be controlled by adjustments made at very low power levels. Third, several high power oscillators can share the same low power driver, which is usually simple and available at low cost.

Injection locking, however, requires high power oscillators with good mode and frequency stability, and with a pulse length longer than the phase-locking time. This paper describes the operation of such a long-pulse relativistic magnetron oscillator system and its injection-locking. Section II describes the apparatus used in the experiment. Section III discusses the general operating characteristics of the free running relativistic magnetron (III.A) and the results of the phase locking experiment (III.B). Section IV summarizes the main results of the phase locking study.

### II. APPARATUS

The transformer-based high power modulator produces up to 500 MW, 2  $\mu$ s pulses with a repetition rate of 5 Hz.<sup>10</sup> The high voltage pulses are delivered through the cathode shank to the magnetron diode. The relativistic magnetron diode is located at the center of the bore of a superconducting magnet capable of generating uniform DC fields up to 22 kG. Microwave output is extracted radially in waveguide through the radial access holes in the superconducting magnet. The experimental parameters are listed in Table

I. The magnetron diode (SM2) has a large A-K gap (1.35 cm) to prevent gap-closure and to enhance the power handling capability of the structure. A thick velvet washer (5 mm) is chosen for the phase locking experiment. Thicker cathodes have longer lifetimes and sustain the 2D-mode structure better than thin washers.

### III. EXPERIMENTAL RESULT

#### A. Operating characteristics

Figure 1 shows the time dependence of output microwave and the corresponding magnetron voltage. The microwave duration ranges from 200 to 400 ns. The impedance of the magnetron diode varies slowly with time, and no signs of impedance collapse (on the fast time scale) are observed. Microwaves are generated at the onset of the radial current, which is about 300–400 A. Typical peak powers are between 20 and 30 MW. The efficiency, namely the output power normalized to the total electron beam power, is about 16 percent. The efficiency can be improved by reducing the axial current.

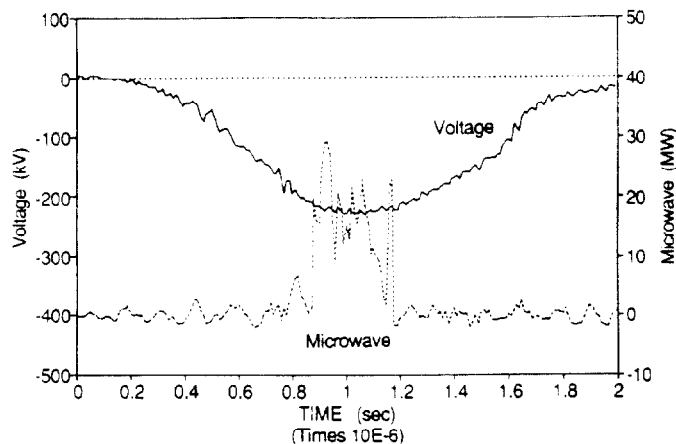


Figure 1 Operating characteristics of a free-running SM-2 magnetron.

#### B. Phase locking result

The layout of the phase-locking experiment is shown schematically in figure 2. Microwave radiation is extracted from the interaction region through a high power circulator with 20 dB isolation. The power from the tunable 1 MW RF driver is injected through the same circulator into the main oscillator. A 20 dB isolator is placed between the driver and the circulator so that the overall isolation is 40

dB. The isolation prevents the driver from being locked by RM's leakage power.

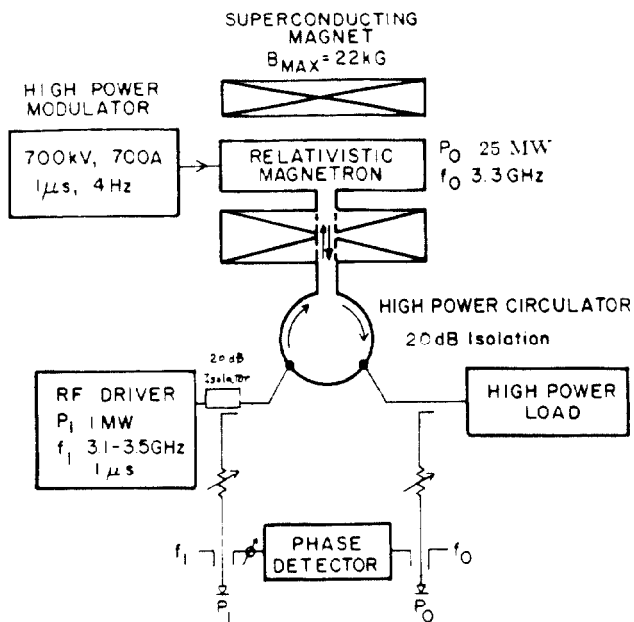


Figure 2 Schematic of the phase-locking experiment.

Clear signs of phase locking are observed. Figure 3 is an example of such a phase-locked shot. The driver signal  $P_i$  (middle trace) is monitored before injection into the circulator. The upper trace shows the high power RF from the RM riding on top of a low power injection plateau. The bottom trace in figure 3 shows the evolution of the relative phase. During the absence of the RM signal (for example, in the time interval between 0.9 and 1.1  $\mu$ s) the phase detector measures the relative phase between the driver signal and its own image – the low power plateau. The result is a relative phase constant in time. We use this as a reference state at  $0^\circ$ . When the RM turns on at 1.15  $\mu$ s, the relative phase is pulled to a new angle at  $12^\circ$ . This new phase angle is reproducible from shot to shot and defines a phase locked state which relaxes back to the reference state at  $0^\circ$  when the RM is off. By using a

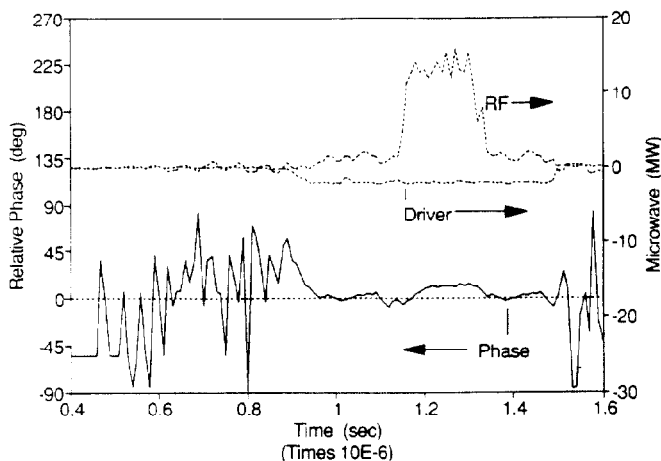


Figure 3 Example of a phase-locked shot.

stringent criterion of  $\pm 3^\circ$  to define the phase-locked states, typically the locked duration is between 100 and 300 ns. The shot-to-shot reproducibility of the final locked phase angle is better than  $\pm 2^\circ$ .

The results of a large number of experiments involving various injection frequencies (ranging from -10 MHz to 10 MHz) and injection power ratios (ranging from 1:1000 to 1:10) are compiled in figure 4. The solid squares in the figure stand for the cases phase-locked states are identified. The blank squares represent those cases when no phase-locking occurs. A magnetron-specific phase-locking model was developed in reference 6 using the standard equivalent-circuit approach and takes into account the frequency pushing effect. The model predicts a locking-bandwidth wider than that in conventional locking theory

$$\Delta\omega \leq \frac{\omega_0}{2Q \cdot \cos\alpha} \cdot \sqrt{\frac{P_i}{P_o}}$$

In the equation,  $\Delta\omega$  is the locking frequency range,  $\omega_0$  is the free-running oscillator frequency,  $\alpha$  is the frequency pushing parameter,<sup>6</sup> and  $P_o$  and  $P_i$  are the oscillator output and input power, respectively. The  $1/\cos\alpha$  factor is attributed to the frequency pushing effect in RMs.

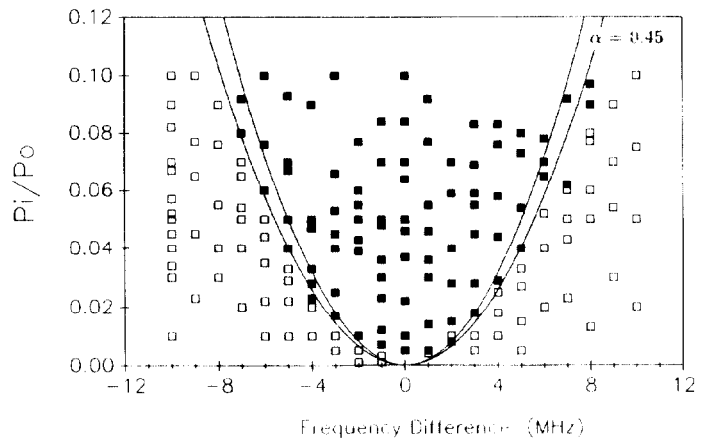


Figure 4 Map of the phase-locking zone.

The two solid curves in figure 4 are the locking zone boundaries predicted by (1) the Adler's condition with frequency pushing effect correction and (2) the Adler's condition alone. The data points are consistent with the theory curve described by the above equation with a pushing parameter  $\alpha$  of 0.45.<sup>6</sup>

The magnitude of frequency pushing is also confirmed in an independent measurement of the final phase. In figure 5, the dependence of the final locked-phase on the injection power and frequency is mapped out. The cases for 5 injection frequencies (-4MHz, -2MHz, 0MHz, 2MHz, and 4MHz) are shown for various injection power ratios (1:1000 to 1:10). Again, the data points agree well with the theory with a frequency pushing parameter  $\alpha$  of 0.45.

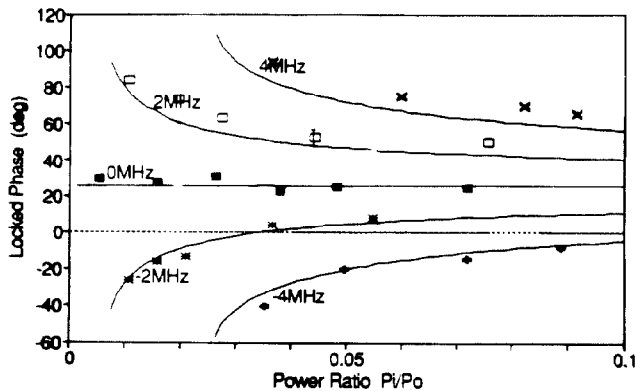


Figure 5 The dependence of the final locked-phase on the injection power and injection frequency difference.

#### IV. CONCLUSION

We have phase locked an S-band (3.3 GHz) long-pulse high power relativistic magnetron oscillator (400 ns at 25 MW) by external injection (20 kW - 1 MW). A reproducible final phase-locked angle is achieved with an injection power ratio as low as 1:200. The phase stability of the phase-locked states is  $\pm 3^\circ$  degrees throughout the 300 ns pulse.

Parametric study of the phase-locked states reveals the importance of frequency pushing effect in phase-locking. The measured locking bandwidth agrees well with the theory which takes into account the frequency pushing effect. The measured dependence of final locked phase on  $\Delta\omega$  and  $P_i/P_o$  also agrees well with theory.

#### V. ACKNOWLEDGEMENT

This work was supported by Strategic Defense Initiative Organization, Office of Innovative Science and Technology, and managed by Harry Diamond Laboratories.

#### VI. REFERENCE

1. S.C. Chen, G. Bekefi, and R.J. Temkin, "Operation of a long-pulse relativistic magnetron in a phase-locking system," H.E. Brandt, Editor, *Proc. SPIE*, vol. 1226, pp. 36-43, 1990.
2. S.C. Chen, G. Bekefi, R. Temkin, and C. de Graff, "Proposed injection locking of a long pulse relativistic magnetron," H.E. Brandt, Editor, *Proc. SPIE*, vol. 1061, pp. 157-160, 1989.
3. S.C. Chen and G. Bekefi, "Relativistic magnetron research," N. Rostoker, Editor, *Proc. SPIE*, vol. 873, pp. 18-22, 1988.
4. J. Benford, H.M. Sze, W. Woo, R.R. Smith, and B. Harteneck, "Phase locking of relativistic magnetrons," *Phys. Rev Lett.*, vol. 62, pp. 969-971, 1989.
5. T.A. Treado, R.S. Smith III, C.S. Shaughnessy, and G.E. Thomas, "Temporal study of long-pulse relativistic magnetron operation", *IEEE Trans. on Plasma Science*, vol. 18, pp. 594-602, 1990.
6. S.C. Chen "Growth and frequency pushing effects in relativistic magnetron phase-locking", *IEEE Trans. on Plasma Science*, vol. 18, pp. 570-576, 1990.
7. G.L. Johnston, S.C. Chen, R.C. Davidson, and G. Bekefi, "Models of driven and mutually-coupled relativistic magnetrons with nonlinear frequency-shift and growth-saturation effects", H.E. Brandt, Editor, *Proc. SPIE*, vol. 1407 (in this volume), 1991.
8. G.L. Johnston, S.C. Chen, R.C. Davidson, and G. Bekefi, "Models of driven relativistic magnetrons with nonlinear frequency-shift and growth-saturation effects", H.E. Brandt, Editor, *Proc. SPIE*, vol. 1226, pp. 108-116, 1990.
9. W. Woo, J. Benford, D., Fittinghoff, B. Harteneck, D. Price, R. Smith, and H. Sze, "Phase locking of high-power microwave oscillators," *J. Appl. Phys.*, vol. 65, pp. 861-866, 1989.
10. W. Mulligan, S.C. Chen, G. Bekefi, B.G. Danly, and R.J. Temkin, "A high-voltage modulator for high-power rf source research", *IEEE Trans. on Elec. Dev.*, to be published in April, 1991.